

# AN ANALYTIC SOLUTION FOR KERNEL ADAPTIVE FILTERING

Benjamin Colburn\*, Luis G. Sanchez Giraldo†, Kan Li\*, and Jose C. Principe\*

\*University of Florida, †University of Kentucky

## ABSTRACT

Conventional kernel adaptive filtering (KAF) uses a prescribed, positive definite, nonlinear function to define the Reproducing Kernel Hilbert Space (RKHS), where the optimal solution for mean square error estimation is approximated using search techniques. Instead, this paper proposes to embed the full statistics of the input data in the kernel definition, obtaining the first analytical solution for nonlinear regression and nonlinear adaptive filtering applications. We call this solution the Functional Wiener Filter (FWF). Conceptually, the methodology is an extension of Parzen's work on the autocorrelation RKHS to nonlinear functional spaces. We provide an extended functional Wiener equation, and present a solution to this equation in an explicit, finite dimensional, data-dependent RKHS. We further explain the necessary requirements to compute the analytical solution in RKHS, which is beyond traditional methodologies based on the kernel trick. The FWF analytic solution to the nonlinear minimum mean square error problem has better accuracy than other kernel-based algorithms in synthetic, stationary data. In real world time series, it has comparable accuracy to KAF but displays constant complexity with respect to number of training samples. For evaluation, it is as computationally efficient as the Wiener solution (with a larger number of dimensions than the linear case). We also show how the difference equation learned by the FWF from data can be extracted leading to system identification applications, which extend the possible applications of the FWF beyond optimal nonlinear filtering.

## 1. INTRODUCTION

Norbert Wiener's 1949 work on minimum mean square estimation (MMSE) initiated the theory of optimum filtering [34]. The mathematics to solve integral equations, the Wiener-Hopf method [36], were crucial to arrive at the optimal parameter function, however, the methodology is rather complex. In digital signal processing using finite impulse response filters, the Wiener solution coincides with least squares, as proven by the Wiener-Khinchin theorem [35]. Unfortunately, the solution still belongs to the span of the input

This material is based upon work supported by the Office of the Under Secretary of Defense for Research and Engineering under award numbers N00014-21-1-2295 and N00014-21-1-2345.

data i.e., the corresponding filter is linear in the parameters and therefore it is not a universal functional approximator.

In the late 50's, Emmanuel Parzen [22] presented an alternative approach to solve the MMSE problem in a Reproducing Kernel Hilbert Space (RKHS) defined by the autocorrelation function of the data. The history of RKHS applications started in physics (Fredholm equations), statistics, signal processing, and machine learning [32, 13, 12, 8]. Here, it will also be clear that the RKHS framework provides a natural link between stochastic processes and deterministic functional analysis.

Parzen's essential idea is that there exists a congruence map between the set of random variables spanned by the random process  $\{X_t, t \in T\}$  with covariance function  $R(t, s) = \mathbb{E}[X_t X_s]$  and the RKHS of vectors spanned by the set  $\{R(\cdot, t), t \in T\}$  denoted as  $\mathcal{H}_R$ . Note that the kernel estimates the second-order statistics of the data (a data-dependent kernel). Parzen clearly states that this RKHS offers an elegant functional analysis framework for MMSE solutions such as regression [7], least squares estimation of random variables, detection of signals in Gaussian noise [6], and others. Unfortunately, the autocorrelation kernel is a linear kernel, so  $\mathcal{H}_R$  yields only linear solutions to the regression problem. Parzen's beautiful interpretation did not provide any practical improvement, so it was forgotten in signal processing.

This paper takes Parzen's work one step further by defining an analytic solution for the Wiener filter in a space nonlinearly related to the input space, which is novel as far as we know. Using analogous techniques to Parzen's work in [22] we create a data-dependent kernel based on the covariance function of projected feature vectors in a space nonlinearly related to the input space. The end result is an analytic solution to optimal nonlinear filters for strictly stationary signals. The proposed approach differs significantly from current kernel adaptive filtering (KAF) [16] [20], where a weighted sum of functionals centered at individual samples approximate the MMSE using search techniques. While a closed-form solution for a nonlinear filter is interesting in its own right, the idea of embedding the statistics of input data, its internal dependency structure, into the inner product structure of an RKHS defined by a nonlinear kernel is perhaps the more general and important contribution of this work, with many applications in science and engineering.

In order to achieve our goals, full access to the structure

of the RKHS is necessary, which is beyond the conventional “kernel trick” [29]. Since the kernel in our case preserves the statistical time structure of the input random process (or of the multivariate random variable), one needs the flexibility of an operator which includes time beyond the simple inner product between two projected samples. For this reason, we approximate the kernel by an explicit, finite dimensional RKHS. In the case of the Gaussian kernel, the RKHS is defined by Hermite-Gaussian functions of a certain dimension selected by the user, as suggested in [17]. The advantage is that the inner product becomes an explicit quadratic form, which allows for much more control of the projections. The disadvantage is that the explicit RKHS is finite dimensional i.e., no longer universal, but the dimensionality is under control of the user. The previous results [17] show that excellent approximations for adaptive filters are obtained with just 20 – 50 dimensions.

The rest of the paper will continue as follows. In section II, we give a brief review of optimal linear filtering in an RKHS. Then in section III we will describe the extension of this idea to a space defined by a nonlinear kernel, which gives rise to the Functional Wiener Filter (FWF). In section IV the analytic FWF solution is described, followed by the algorithmic solution applied to data samples. We also present an error analysis of the FWF. In section V we discuss how to recover a difference equation from the FWF showing that the method has application beyond just optimal nonlinear filtering. We then compare the performance of the FWF with KAF and other nonlinear filtering methods (Gaussian Processes and Kernel Ridge Regression) and give experimental validation of FWF even for non-stationary time series. Section VI summarizes the paper and compares the methodology with KAF. In the appendix we give an explanation of why previous attempts in [3] and [4] were unsuccessful when compared to this derivation of the FWF.

## 2. REVIEW OF LINEAR FILTERING OF CONTINUOUS TIME SERIES IN RKHS

Let  $\mathcal{X}$  be a non-empty set, and  $K(x, x')$  a function defined on  $\mathcal{X} \times \mathcal{X}$  that is non-negative definite. The Moore-Aronszajn theorem [1], guarantees that  $K(x, x')$  defines uniquely a RKHS,  $\mathcal{H}_K$ , such that  $K(\cdot, x) \in \mathcal{H}_K$  and for any  $g \in \mathcal{H}_K$ , yields  $\langle g, K(\cdot, x) \rangle_{\mathcal{H}_K} = g(x)$ . Therefore, an RKHS is a special Hilbert vector space associated with a kernel such that it reproduces (via the inner product) in the space, i.e.,  $\langle K(\cdot, x), K(\cdot, x') \rangle_{\mathcal{H}_K} = K(x, x')$ ; or equivalently, a space where every point evaluation functional is bounded.

A stochastic process  $\{X_{t,\omega}, t \in T\}$  is broadly defined as a collection of random variables(r.v) on a measurable sample space  $(\Omega, \mathcal{B}_\Omega)$ , indexed by a set  $T$ . Here, we restrict  $X_{t,\omega}$  to random variables taking values in  $\mathbb{R}$ , and  $T \subset \mathbb{R}$ , which we call a time-series,  $\{X_t, t \in T\}$  and omit the dependence on  $\omega$  for simplicity. We can further simplify the notation and write  $\{X_t, t \in T\}$  as  $\{X_t\}$ . For a time-series with finite sec-

ond order moments, let  $L_2(\{X_t\})$  denote the space of all real valued random variables spanned by the time series i.e., this space consists of all r.v. that are either linear combinations of finite number of  $\{X_t\}$  or are limits of such linear combinations.

The time structure is quantified by the joint probability density  $p(X_t, X_s)$  of the pair of random variables,  $X_t$  and  $X_s$ , or a random process sampled at two points in time  $t$  and  $s$ . Assuming a strictly stationary stochastic model for  $X_t$ , the marginal density  $p_{X_t}(x)$  is the same for any  $t$ . Normally, the joint density  $p(X_t, X_s)$  is quantified by its mean value, called the autocorrelation function. To simplify notation, let us define the time autocorrelation of the time series as:

$$R(s, t) = \mathbb{E}[X_s X_t]. \quad (1)$$

The autocorrelation function on time sample pairs is positive semi-definite, hence by Moore-Aronszajn theorem [1] it defines a RKHS space of functions on  $T \times T$ , denoted  $\mathcal{H}_R$ . Notice that the inner product in  $\mathcal{H}_R$  depends on the statistics of the data through  $X_t$ , while the functions in  $\mathcal{H}_R$  are deterministic because of the  $\mathbb{E}[\cdot]$  operator.

For any pair of random variables  $A, A' \in L_2(\{X_t\})$ , define their inner product as

$$\langle A, A' \rangle = \mathbb{E}[AA'] \quad (2)$$

and the induced norm of  $A$  in  $L_2(\{X_t\})$  by  $\langle A, A \rangle = \mathbb{E}[A^2]$ . Obviously, this inner product coincides with the autocorrelation function if  $A$  is  $X_s$  and  $A'$  is  $X_t$ . However, notice that  $L_2(\{X_t\})$  is not an RKHS.

### 2.1. Explicit Expression for MMSE

One of the important problems in time series analysis is the representation of an unobservable r.v.  $Z$ . Let  $\{X_t, t \in T\}$  be an observable time series assumed stationary. The goal is to create a linear combination of the observable time series that has the smallest mean squared distance to  $Z$ . By the Hilbert projection theorem, there is a unique minimum norm projection between the abstract Hilbert space  $\mathcal{H}$  and any subspace  $\mathcal{M}$  of  $\mathcal{H}$ . Then, there exists a unique vector  $A^*$  in  $\mathcal{M}$ , given by  $A^* = \mathbb{E}^*[A|\mathcal{M}]$ , which is the orthogonal projection of a vector  $A$  in  $\mathcal{H}$  to  $\mathcal{M}$ . For a family of vectors  $\{X_t, t \in T\}$  the projection becomes

$$A^* = \mathbb{E}^*[A|X_t, t \in T]. \quad (3)$$

Then with  $A = Z$ , the optimal linear predictor is the unique r.v. in  $L_2(\{X_t\})$  that satisfies

$$\mathbb{E}[\mathbb{E}^*[Z|X_t, t \in T]X_s] = \mathbb{E}[ZX_s] \quad (4)$$

for any  $s \in T$ . This result gives immediately rise to the famous Wiener equation. Indeed, if  $T$  is a finite interval  $T = \{t : a \leq t \leq b\}$  and  $w(t)$  a weighting function in  $L_2$ , the integral

$$\int_a^b X(t)w(t)dt \quad (5)$$

represents a r.v. in  $L_2(X_t, t \in T)$ , then the weighting function of the best linear predictor can be written as

$$\mathbb{E}^*[Z|X_t, t \in T] \triangleq \int_a^b X(t)w^*(t)dt \quad (6)$$

and must satisfy the generalized Wiener equation

$$\int_a^b w^*(t)R(s,t)dt = \rho_z(s) \quad (7)$$

in  $a \leq s \leq b$ , with  $R(s,t) = \mathbb{E}[X_s X_t]$ , and  $\rho_z(s) = \mathbb{E}[ZX_s]$ .

This result states that one can always find a representation for the function  $\rho_z(s)$  in terms of the functions  $\{R(s,t), t \in T\}$  such that the MMSE linear predictor  $\mathbb{E}^*[Z|X_t, t \in T]$  can be written in terms of the corresponding linear operator on the time series  $\{X_t, t \in T\}$ .

Parzen showed that the solution of the prediction problem may be written as follows [22]. If  $Z$  is a r.v. with finite second moments and  $\rho_z(s) = \mathbb{E}[ZX_s]$  then

$$\begin{aligned} \rho_z &\in \mathcal{H}_R \\ \mathbb{E}^*[Z|X_t, t \in T] &= \langle \rho_z, X \rangle_{\mathcal{H}_R}. \end{aligned} \quad (8)$$

The equivalent MMSE solution in the data space becomes,

$$\begin{aligned} Y &= \mathbb{E}^*[Z|X_t, t \in T] = \langle \rho_z, X \rangle_{\mathcal{H}_R} \\ &= \int_{t \in T} \int_{s \in T} R^{-1}(s,t) \rho_z(s) X(t) ds dt \end{aligned} \quad (9)$$

which coincides with the Wiener solution  $\int_{t \in T} X(t)w^*(t)dt$ . Furthermore, in digital signal processing the double integral becomes a double sum and it can be computed in the input space directly from samples as

$$\begin{aligned} Y(t) &= \langle X_t, R^{-1} \rho_z \rangle_{L_2} = \langle X_t, \rho_z \rangle_{\mathcal{H}_R} \\ &= \sum_{t=0}^{L-1} \sum_{s=0}^{L-1} X(t) R^{-1}(s,t) \rho_z(s). \end{aligned} \quad (10)$$

Note that the autocorrelation matrix and the cross-correlation vector must be first estimated from a training set. Another interesting fact is that the dimension of  $\mathcal{H}_R$  is the number of delays, which is under user control. Moreover, in  $\mathcal{H}_R$  this solution is coordinate free, does not use the approximation error, and directly uses the structure of  $\mathcal{H}_R$ . In fact, it is sufficient to compute the linear projection between  $\rho_z(s)$  with the input data because the covariance kernel  $R(s,t)$  is implicit in the inner product of  $\mathcal{H}_R$ , unlike Wiener-Hopf method that requires spectral factorization. This coordinate free property of RKHS solutions with the covariance kernel was first noted

by Loèeve [21] who suggested that, instead of finding a set of functional projections (e.g. Karhunen-Loèeve Transform), it is sufficient to employ the statistics of  $\{X_t\}$  embedded in the structure of the RKHS. Parzen [22] further states that for this reason “RKHS defined by the covariance kernel is the natural setting in which to solve problems of statistical inference on time series”.

The fundamental issues with Parzen approach are twofold: first, it does not elucidate efficient alternatives to implement the conditional mean operator; second, for discrete time signal processing, this approach is computationally more complex than the famous Wiener solution  $w^* = R^{-1}\rho$ , where  $R$  is the autocorrelation matrix (the kernel  $R(s,t)$  evaluated at a finite set of delays), and  $\rho$  is the cross-correlation vector.

We conclude that the advantage of the RKHS theory is on the mathematical tools of congruence and representation of time series in RKHS, which opens the door to seek analytical solutions for nonlinear regression. A key feature of the RKHS theory is that functionals defined in the RKHS are independent of the kernel utilized, therefore we can expect that a similar form to (9), which finds a minimum norm projection for nonlinear regression, exists in a different RKHS. Hence, the key goal for nonlinear extensions of Parzen’s approach is to concentrate on designing proper kernels and more general frameworks based on operators.

### 3. THE NONLINEAR PREDICTION CASE

Our goal now is to define a novel RKHS that preserves the correlation structure defined by the data, as done in  $\mathcal{H}_R$ , but also maps the time series by a nonlinear kernel to achieve Convex Universal Learning Machine (CULM) properties [23]. There are several ways we could proceed. Perhaps the most straight forward is to define an RKHS with a kernel that extends the autocorrelation function [38], called correntropy [18], which is also a positive definite function of two arguments defined in a Gaussian RKHS. Unfortunately, this route lead to the need for heuristic approximations which yields poor generalization as mentioned in [4] and [3].

As an alternative, here we define and apply an operator that analytically computes the minimum norm projection in an explicit finite dimensional RKHS that approximates the Gaussian RKHS i.e.

$$G_\sigma(\mathbf{x}, \mathbf{x}') : \mathcal{X} \times \mathcal{X} \rightarrow \mathbb{R} \approx \hat{\phi}(\mathbf{x})^T \hat{\phi}(\mathbf{x}') \quad (11)$$

where  $\mathcal{X} = \mathbb{R}^p$ , with mapping  $\hat{\phi} : \mathcal{X} \rightarrow \mathbb{R}^D$ ,  $G_\sigma$  is the Gaussian function with kernel size  $\sigma$ ,  $p$  is the dimension of the input data, and  $D$  is the number of dimensions in the finite RKHS. The definition of a nonlinear, but finite dimensional RKHS makes this task much easier, while with a controlled error.

In [17] the explicit mapping function based on the Taylor expansion of the Gaussian kernel is used to define a finite

dimensional RKHS which approximates the feature space defined by the Gaussian kernel. A more in depth discussion can be found in [5]. This is just one way of getting an explicit feature space; another notable technique employs random Fourier features (RFF) [26], but it is a more computationally expensive method than the Taylor expansion based method. The advantage of the explicit RKHS is that we can employ directly linear operators in the feature space, which provides much more flexibility when compared with the kernel trick. We will refer to the explicit finite rank feature space as  $\mathcal{H}_B$ , with kernel  $B(\cdot, \cdot)$ . The explicit mapping function for vectors given in [5] (see also [40, 39]) is given by

$$\phi_{d,j}(\mathbf{x}) = e^{-\frac{\|\mathbf{x}\|^2}{2\sigma^2}} \frac{1}{\sigma^d \sqrt{d!}} \prod_{i=1}^d \mathbf{x}_{j_i}, \quad (12)$$

where  $j \in [p]^d$  enumerates over all selections of  $d$  coordinates of  $\mathbf{x}$  (allowing repetitions and enumerating over different orderings of the same coordinates). For instance, the set  $[2]^3$  consists of eight 3-tuples, namely,  $(1, 1, 1)$ ,  $(1, 1, 2)$ ,  $(1, 2, 1)$ ,  $(1, 2, 2)$ ,  $(2, 1, 1)$ ,  $(2, 1, 2)$ ,  $(2, 2, 1)$ , and  $(2, 2, 2)$ . The finite rank kernel  $B$  is obtained by truncating the series to the first  $k$  terms

$$\begin{aligned} B(\mathbf{x}, \mathbf{x}') &= \left\langle \hat{\phi}(\mathbf{x}), \hat{\phi}(\mathbf{x}') \right\rangle_{\mathcal{H}_B} \\ &= \sum_{d=0}^k \sum_{j \in [p]^d} \phi_{d,j}(\mathbf{x}) \phi_{d,j}(\mathbf{x}') \\ &= e^{-\frac{\|\mathbf{x}\|^2}{2\sigma^2}} e^{-\frac{\|\mathbf{x}'\|^2}{2\sigma^2}} \sum_{d=0}^k \frac{(\mathbf{x}^T \mathbf{x}')^d}{\sigma^{2d} d!}. \end{aligned} \quad (13)$$

It's important to note that the Gaussian kernel is obtained when  $k$  (the number of terms) approaches infinity. However, due to the exponential decay of the Gaussian function's eigenvalues, a good finite rank approximation can often be obtained with just a few terms in the expansion [17].

Normally algorithms which employ RKHSs are written in terms of weighted sums of kernels, and the underlying eigenvalues and eigenfunctions which form a basis for the RKHS are not considered in detail. When we define explicitly the basis of the RKHS we are really treating the RKHS more like a Hilbert space for which we define a basis. Later we will see that it is necessary to work with individual eigenfunctions of the RKHS if we want to define an analytical MMSE solution. Therefore the explicit kernel provides an elegant way of performing the operations necessary for an analytical solution.

### 3.1. Retaining Time Structure in $\mathcal{H}_B$

We can retain the time structure of a stochastic process,  $\{X_t, t \in T\}$ , by applying the finite rank kernel  $B(\cdot, \cdot)$ . This forms the span of the set of random elements,  $\{B(X(t), \cdot), t \in T\}$  taking values in  $\mathcal{H}_B$ . We call this set  $\mathcal{H}_{RB}$ . We can form collections of elements from  $\mathcal{H}_{RB}$  by selecting different time

instances. The inclusion of this set of time indices allow for the quantification of the time structure of the projection of a time series  $\{X_t\}$  into  $\mathcal{H}_{RB}$ . In this collection of elements, we can define functionals based on both time and also across the dimensions of  $\mathcal{H}_{RB}$  (i.e. space), which would require projections defined based on samples using kernel trick.

In order to explain the added flexibility, we give an example here. FIR time filters operate with a finite window of signal samples of  $X(t)$ . Let  $\mathbf{x}_t = [X(t), \dots, X(t - (L - 1))]^T$  be a window of size  $L$ . This window projected into  $\mathcal{H}_{RB}$  has the following form:

$$\phi(\mathbf{x}_t) = \begin{bmatrix} | & & \dots & | \\ \phi(X(t)) & \dots & \phi(X(t - (L - 1))) \\ | & & \dots & | \end{bmatrix}_{D \times L} \quad (14)$$

The resulting collection of random elements is a rank 2 tensor in  $\mathcal{H}_{RB}$  containing elements indexed by time instances  $t$  and spatial indices of  $D$ . Note that many calculations involving  $\mathcal{H}_{RB}$  can be simplified by vectorizing the tensor given in (14). This vectorization is done by stacking each column on top of one another to form a vector in  $\mathbb{R}^{D \cdot L}$ . We will refer to this vectorized version as  $\phi(\mathbf{x}_t)$ .

In most practical cases the user will define both the window size ( $L$ ) and the number of dimensions ( $D$ ) of  $\mathcal{H}_B$ , which in turn defines the dimensions of elements in  $\mathcal{H}_{RB}$ . Note that since we use an explicit mapping function, we have the ability to operate with specific time and space coordinates of elements in  $\mathcal{H}_{RB}$ . When computing the kernel trick in KAF, we only have access to the columns of the matrix, which for the Gaussian kernel are infinite dimensional.

For example, KLMS [19], which is a nonlinear filter, operates with weighted sums of  $G(\mathbf{x}_t, \mathbf{x}_i)$  where  $\mathbf{x}_t$  is the  $L$ -tap vectors including the current input and  $\mathbf{x}_i$  are training samples (also vectors of size  $L$ ). The correntropy function, defined as  $V(t, s) = \mathbb{E}_{t,s}[G(X(t), X(s))]$  can also be computed directly from samples. It is shown in [18] that  $V$  is a similarity metric that contains all the even moments of the joint probability density function  $p_{t,s}(x_t, x_s)$ , which means that autocorrentropy is a measure of statistical dependence [27]. Both examples show the power of RKHS theory, but they don't make explicit use of the eigenstructure of the RKHS. For instance, suppose that we want to estimate the similarity between the first and second dimensions for a given coordinate system in the RKHS. These types of functionals are cumbersome to deal with using the kernel trick as each of these dimensions would have to be expressed as the weighted sum of kernel functions. This would quickly become computationally infeasible. In the Appendix we explain why this type of functional is needed to derive closed-form MMSE solutions.

### 3.2. Correntropy in $\mathcal{H}_{RB}$

In this section we will define an extension to the autocorrelation function  $R(s, t)$  in the space of random elements  $\mathcal{H}_{RB}$ . We will start by defining a tensor based covariance function,  $U_{d_1, d_2}(t, s)$  working on pairs of time and spatial dimensions, as follows:

$$U_{d_1, d_2}(t, s) = \mathbb{E}_{(t, s)}[\phi_{d_1}(X_t)\phi_{d_2}(X_s)] \quad (15)$$

This function selects the dimensions  $d_1$  and  $d_2$  of the explicit mappings to the RKHS of the time series at times  $t$  and  $s$  and then computes their correlation. Equation (15) describes how to calculate one element in the  $U$  tensor. Looping through all space indices will yield the tensor  $U(t, s)$ . We will refer to (15) as the moment-wise correntropy function, because it is a decomposition of the correntropy function described in [18]. Note that if the time series is strictly stationary, then we can combine the pair of time indices into a single index,  $\tau = t - s$  and rewrite  $U$  as

$$U_{d_1, d_2}(\tau) = \mathbb{E}_{t, t-\tau}[\phi_{d_1}(X(t))\phi_{d_2}(X(t-\tau))] \quad (16)$$

If the process is also ergodic, we can estimate  $U$  directly from training samples (realizations of  $\{X_t\}$ ) as

$$\hat{U}_{d_1, d_2}(\tau) = \frac{1}{N} \sum_{t=1}^N \phi_{d_1}(X(t))\phi_{d_2}(X(t-\tau)) \quad (17)$$

where  $N$  is the number of training samples. If we fix  $L$  and  $D$  then we can represent  $U$  as a  $D \times L \times D \times L$  shaped tensor where  $(U)_{d_1, t, d_2, t-\tau} = (U)_{d_2, t+\tau, d_1, t}$ . While this tensor view of the moment-wise correntropy in  $\mathcal{H}_{RB}$  makes clear the idea of measuring correntropy across both time and space, we can create a rank two tensor representation of this function which is easier to work with both in terms of mathematical notation and practical computation. This rank two tensor (or matrix) is just the unfolded version of the  $U$  tensor which is a  $(D \cdot L) \times (D \cdot L)$  matrix. This unfolding is a mode-2 unfolding of the the tensor  $U$  as described in [25], and will be denoted as  $U_M$ . Note that if  $D \rightarrow \infty$ , then the trace of  $U_M$  is exactly equal to the correntropy function introduced in [18] and utilized in [2] and [41].

**Theorem 1.** *The moment-wise correntropy function of random vectors is positive semi-definite (PSD).*

*Proof.* Consider a random vector,  $\mathbf{x}$ , whose realizations take values in  $\mathbb{R}^L$ . Let  $\phi(\mathbf{x})$ , be another random vector in  $\mathbb{R}^{D \cdot L}$  which is the result of applying the vectorized version of the explicit mapping function given in (14). Then its covariance function,  $U_M$ , is defined as  $U_M = \mathbb{E}[\phi(\mathbf{x})\phi(\mathbf{x})^T]$ . Let  $\mathbf{z}$  be an arbitrary real valued random vector with dimension  $D \cdot L$ .

If we show that  $\mathbf{z}^T U_M \mathbf{z} \geq 0$  then  $U_M$  is PSD.

$$\begin{aligned} \mathbf{z}^T U_M \mathbf{z} &= \mathbf{z}^T \mathbb{E}[\phi(\mathbf{x})\phi(\mathbf{x})^T] \mathbf{z} \\ &= \mathbb{E}[\mathbf{z}^T \phi(\mathbf{x})\phi(\mathbf{x})^T \mathbf{z}] \\ &= \mathbb{E}[(\mathbf{z}^T \phi(\mathbf{x}))(\mathbf{z}^T \phi(\mathbf{x}))^T] \end{aligned} \quad (18)$$

Since the inner product  $Y = \mathbf{z}^T \phi(\mathbf{x})$  is a real scalar valued r.v., then

$$\mathbb{E}[(\mathbf{z}^T \phi(\mathbf{x}))(\mathbf{z}^T \phi(\mathbf{x}))^T] = \mathbb{E}[Y^2] \geq 0. \quad (19)$$

□

**Theorem 2.** *If a matrix  $U_M$  is PSD so is its pseudo-inverse<sup>1</sup>*

*Proof.* Let  $U_M$  be a PSD matrix. Then it has an eigendecomposition  $U_M = Q^T \Lambda Q$ . Where  $Q$  contains the orthonormal eigenvectors of  $U$ , and  $\Lambda$  is a diagonal matrix with non-negative real eigenvalues. Then, its pseudo-inverse can be obtained as follows

$$U_M^\dagger = Q \Lambda^\dagger Q^T. \quad (20)$$

Where the entries in the diagonal of  $\Lambda^\dagger$  are the reciprocals of non-negative real numbers defined as  $1/x$  for  $x > 0$  and 0 for  $x = 0$ , and are therefore also non-negative real numbers. Then  $U_M^\dagger$  has only non-negative real eigenvalues and is therefore also PSD. □

Theorem 1 proves that  $U$  is PSD and therefore it can be used to define a RKHS. If we consider the vectorized version of the explicit mapping function,  $\phi(\mathbf{x}_t)$ , then the unfolded version of  $U$  is the moment-wise correntropy function of real valued random vectors.

Furthermore, we can define a new RKHS,  $\mathcal{H}_U$  with the following kernel,

$$K_U(\mathbf{x}, \mathbf{y}) = \phi(\mathbf{x})U_M\phi(\mathbf{y}). \quad (21)$$

where  $\mathbf{x}, \mathbf{y} \in \mathbb{R}^L$  and  $\phi(\mathbf{x}), \phi(\mathbf{y}) \in \mathbb{R}^{D \cdot L}$  are the vector representations of functions in  $\mathcal{H}_{RB}$ .

$K_U$  contains information about the correlations of a time series  $\{X_t, t \in T\}$  projected into  $\mathcal{H}_{RB}$ , and therefore defines a Hilbert space with a data-dependent inner product. However, its important to note that these correlations are functions not just of  $\{X_t\}$ , but also of the eigenfunctions of  $\mathcal{H}_B$ . This is more than a measure of second order statistics (correlation) because it contains the even moments of the probability density function of the input data (up to order  $D$ ) [18].

Rather than defining  $K_U$  by directly estimating its eigen-decomposition, we describe the kernel as an operator over  $\mathcal{H}_{RB}$  where the eigenfunctions of  $\mathcal{H}_{RB}$  are already explicitly known. Since the kernel defining  $\mathcal{H}_B$  is a truncation of the Gaussian kernel, we can only claim universality in the limit. However, we show experimentally that for many applications

<sup>1</sup>We mean the Moore-Penrose pseudo-inverse.

this truncation will still yield very good results in terms of MSE.

To elaborate on how we access the space  $\mathcal{H}_U$ , in many works such as [31] and [28] an integral operator is estimated by finding the leading eigenfunctions and values. Here we do not take this approach. Instead, we use the fact that all separable finite dimensional Hilbert spaces defined on the same domain with the same number of dimensions are isomorphic to  $\mathbb{R}^M$  [14], where  $M$  is the dimension of the space. Therefore, the two Hilbert spaces,  $\mathcal{H}_{RB}$  and  $\mathcal{H}_U$  are isomorphic. We find the isomorphism between these two spaces ( $U^{\frac{1}{2}}$ ) and then use this operator to estimate the kernel function  $K_U$  without ever explicitly defining the eigendecomposition of  $K_U$ . This type of argument can be extended to infinite dimensional spaces by saying that the different separable Hilbert spaces with infinite dimension are isomorphic to  $\ell^2$  the space infinite sequences with finite energy [14]. However, the computation of an operator like  $U^{\frac{1}{2}}$  in an infinite dimensional space is of course impractical. The ability to explicitly define and apply operators is an important strength of finite dimensional RKHSs.

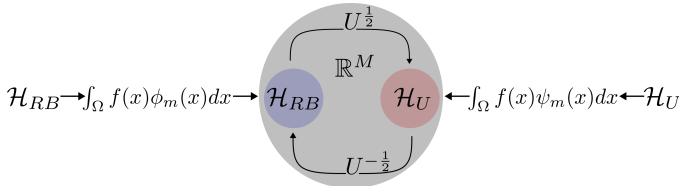


**Fig. 1.** Depiction of the relationship between  $\mathcal{H}_U$  and  $\mathcal{H}_{RB}$ . Note that we never explicitly find the eigenbasis  $\{\psi_m\}_{m=1}^M$ , but we are able to access  $\mathcal{H}_U$  through the kernel function  $U$ .  $M = D \cdot L$ .

#### 4. THE WIENER SOLUTION IN $\mathcal{H}_U$

The MMSE for the linear case is given in (4), where the projection of a desired signal into the linear span of an input signal is found. In the nonlinear case we would like to project a desired signal into the span of the composition of a time series and the feature map given by the kernel of  $\mathcal{H}_B$ ,

$$\mathbb{E}[\mathbb{E}^*[Z|\phi(X_t, t \in T)]\phi(X_s)] = \mathbb{E}[Z\phi(X_s)]. \quad (22)$$

Parzen succinctly states that if one can find a representation of  $\rho_z(s)$  in terms of linear operations on the covariance kernel, then the MMSE linear predictor,  $\mathbb{E}^*[Z|X_t, t \in T]$ , can be written in terms of the corresponding linear operations on the time series. With (22) in mind, we can use this idea to extend the Wiener solution to  $\mathcal{H}_{RB}$ , which is nonlinearly related the input space.

First, we define the cross-covariance function between a random process projected into  $\mathcal{H}_{RB}$  and some r.v.  $Z$  as

$$\rho_d(t) = \mathbb{E}_t[Z\phi_d(X_t)]. \quad (23)$$

where  $d = 1, \dots, D$ . In tasks such as time series prediction if we assume strict stationarity and ergodicity then  $\rho$  becomes a function of only lag ( $\tau$ ) and dimension ( $d$ ).

$$\rho_d(\tau) = \mathbb{E}_{t-\tau}[Z\phi_d(X_{t-\tau})] \quad (24)$$

Notice that if  $\tau = 0, \dots, L-1$  then looping through all values of  $\tau$  will result in a rank two tensor  $(\rho)_{d,\tau}$ , which is a  $D \times L$  tensor containing a scalar weight corresponding to each eigenfunction of  $\mathcal{H}_{RB}$ . In other words it is a function in  $\mathcal{H}_{RB}$  with a similar definition to equation 14.

Practically if we assume  $Z$  takes a scalar value for every  $t \in T$ , then  $\rho$  can be estimated from training data samples as

$$\hat{\rho} = \frac{1}{T} \sum_{t=1}^T Z(t)\phi(\mathbf{x}_t) \quad (25)$$

Note that (25) is given in terms of the vector representation of functions in  $\mathcal{H}_{RB}$ , but  $\hat{\rho}$  can be unfolded to recover the tensor  $(\rho)_{d,\tau}$ . Following Parzen's approach and by analogy with (10), the MMSE solution in the data space is

$$\begin{aligned} \hat{Y}(t) &= \langle \phi(\mathbf{x}_t), \rho \rangle_{\mathcal{H}_U} \\ &= \sum_{n=1}^{D \cdot L} \sum_{m=1}^{D \cdot L} \phi_n(\mathbf{x}_t) U_M^{-1}(n, m) \rho_m \end{aligned} \quad (26)$$

where  $n, m = 1, \dots, (D \cdot L)$  loop through all combinations of time and space indices. Equation (26) is the FWF analytic solution in the data space and an analog to linear solution given in (10). Notice that it is constant complexity, unlike other kernel-based solutions whose complexity increases with respect to training set size. The FWF solution is linear in  $\mathcal{H}_{RB}$ , but nonlinear in the input space. The main difference between this nonlinear solution and its linear counterpart in  $\mathcal{H}_B$  is the addition of an extra spatial dimension gained when we substitute the input data  $X(t)$  with  $\phi(X(t))$ .

We can show the ramifications of adding this spatial dimension to the Wiener equation given in (7). In order to do this we would like to create an analog to equation (7) which describes the problem we implicitly solve when we compute equation (26).

It's important to remember that while  $\phi(\mathbf{x}_t)$  and  $\rho$  are matrices of size  $D \times L$ , they represent spatiotemporal functions. For example, consider some real-valued rank 2 tensor  $V$  of size  $D \times L$ . Let  $\Omega$  be the domain of the eigenfunctions of  $\mathcal{H}_B$ . Then in  $\mathcal{H}_{RB}$   $V$  represents the following function.

$$v(t, x) = \sum_{d=1}^D (V)_{d,t} \phi_d(x) \quad (27)$$

where  $x \in \Omega$ ,  $V_{d,t}$  points to a single scalar valued element of the tensor  $V$ , and  $t = 0, \dots, L-1$  assuming discrete time. Remember that when we take the inner product in  $\mathcal{H}_{RB}$  we

are really taking the sum of  $L$  integrals. For example, consider two real-valued  $D \times L$  tensors  $V$  and  $V'$ . These represent two functions in  $\mathcal{H}_{RB}$ . Then the following statements are equivalent.

$$\begin{aligned} \langle V, V' \rangle_{\mathcal{H}_{RB}} &= \sum_{t=0}^{L-1} \sum_{d=1}^D (V)_{d,t} (V')_{d,t} \\ &= \sum_{t=0}^{L-1} \int_{\Omega} v(t, x) v'(t, x) dx \end{aligned} \quad (28)$$

where  $v(t, x)$  and  $v'(t, x)$  are the spatiotemporal functions defined over the domain  $T \times \Omega$  represented by the tensors  $V$  and  $V'$ .

Now, we will describe the set of integral operators whose matrix representations are stored in the  $U$  tensor. To simplify the description we will assume that some fixed  $L$  and  $D$  have been chosen. Let  $s, t = 0, \dots, L-1$  and  $d_1, d_2 = 1, \dots, D$ . Then let  $\mathcal{U} = \{(U)_{:, :, s, t}, s, t = 0, \dots, L-1\}$ , where the colons  $U_{:, :, s, t}$  denote taking all possible values for  $d_1$  and  $d_2$ . Each element in  $\mathcal{U}$  is a  $D \times D$  matrix and is the matrix representation of an operator which acts on elements in  $\mathcal{H}_B$ . We can rewrite each element in  $\mathcal{U}$  as an integral operator.

$$\mathcal{L}_U^{st}(x, y) = \sum_{d_1=1}^D \sum_{d_2=1}^D (U)_{d_1, d_2, s, t} \phi_{d_1}(x) \phi_{d_2}(y). \quad (29)$$

where  $x, y \in \Omega$  and  $(U)_{d_1, d_2, s, t}$  is a scalar valued element of the tensor  $(U)_{:, :, s, t}$ . Equation 29 gives the integral operator for one element in  $\mathcal{U}$ , so we can store all of these integral operators in another set,  $\mathcal{L}_U = \{\mathcal{L}_U^{st}, s, t = 0, \dots, L-1\}$ . Then  $\mathcal{U}$  and  $\mathcal{L}_U$  are two sets holding different representations of equivalent operators.

Then the equation that is solved implicitly in (26) is

$$\sum_{t=0}^{L-1} \left[ \int_{\Omega} w(t, x) \mathcal{L}_U^{st}(x, y) dx \right] = \rho(s, y) \quad (30)$$

where  $w(t, x)$  and  $\rho(s, y)$  are two spatiotemporal equations defined over the domain  $T \times \Omega$ . When we take the inverse of  $U_M$  and multiply this by the vector representation of  $\rho(s, y)$  we solve for  $\mathbf{w}^*$  which is the vector representation of the spatiotemporal function,  $w^*(t, x)$ , which solves (30). Equation (30) is a direct discrete time analog to equation (7). For this reason we call it the functional Wiener equation.

The differences between equations (7) and (30) appear because we are no longer working with scalar valued functions of time,  $X(t)$ . Rather, we are working with collections of functions indexed by time,  $\phi(\mathbf{x}_t)$ . In the linear case we can think of  $R(s, t)$  as a set of scalars indexed by two time indices. This is sufficient in the linear case, as  $w(t)$  is a scalar valued function of time. In the case of the FWF, the "weights"  $w$  of

the system are spatiotemporal functions i.e., for every time  $t$ ,  $w(t, x)$  is a function over  $\Omega$  not a scalar. Therefore, in order to operate on this function, we need an integral operator (not a single scalar). This is why a second integral is needed over  $\Omega$  which describes the application of an integral operator,  $\mathcal{L}_U^{st}$ , to the function  $w(t, x)$ .

The extension of equation (30) for continuous time can be in principle written as

$$\int_a^b \left[ \int_{\Omega} w(t, x) \mathcal{L}_U^{st}(x, y) dx \right] = \rho(s, y) \quad (31)$$

where  $a \leq s \leq b$ . However, the set  $\mathcal{L}_U$  will become uncountable.

#### 4.1. Calculation of the Function Wiener Filter

Equation (26) shows clearly the extension of Parzen's solution to a space non-linearly related to the input space. However, this form of the solution is not as computationally efficient as it could be. In this section we describe a computationally efficient way to calculate the MMSE solution described above.

We are given some finite number of input signal samples,  $X(i)$ , and desired signal  $Z(i)$  with the goal of mapping windows of  $X(i)$  to its corresponding  $Z(i)$ . Let,  $X = \{\mathbf{x}_i, i \in I\}$  be the set of all windows of time in  $X(i)$  of length  $L$ .  $|I|$  is the number of training windows in  $X(i)$ . Each window of time in this data set can be projected into  $\mathcal{H}_{RB}$  using (14) yielding a  $D \times L$  tensor for each window in time. Then we vectorize these tensors by stacking the columns of this tensor on top of one another to form a vector of length  $D \cdot L$  for each window of time in the training set. Finally, we end up with a data matrix,  $\mathcal{X} = \{\phi(\mathbf{x}_i), i \in I\}$ , which is a  $(D \cdot L) \times |I|$  matrix where each column represents the projection of a window in time into  $\mathcal{H}_{RB}$ . Let  $z_i$  denote the desired value corresponding to the input vector  $\mathbf{x}_i$ . We can store all of these desired values in a vector  $\mathbf{z}_{(I \times 1)}$ . Note that we may use the Moore-Penrose pseudo inverse in the case that  $U_M$  is ill-conditioned.

Then we can calculate the matrix form of  $U$ ,

$$\hat{U}_M = \frac{\mathcal{X}^T \mathcal{X}}{|\mathcal{X}|}. \quad (32)$$

The estimation of the cross-correlation vector is

$$\hat{\rho} = \frac{\mathcal{X} \mathbf{z}}{|\mathcal{X}|}. \quad (33)$$

Where  $\hat{\rho}$  is just the weighted sum of the columns of  $\mathcal{X}$ . Then we can calculate the projection of  $Z$  into  $\phi(\{X_i, i \in I\})$  as

$$\mathbf{w}^* = U_M^{-1} \hat{\rho} \quad (34)$$

Where  $\mathbf{w}^*$  is a vector of size  $(D \cdot L)$  which represents the optimal solution in  $\mathcal{H}_{RB}$ . Lastly, in order to make predictions with this solution we just take the inner product between  $\mathbf{w}^*$

and  $\phi(\mathbf{x}_t)$  in  $\mathcal{H}_{RB}$ . Since we are using an explicit space this is just the inner product between two vectors.

$$\hat{Y}(t) = \langle \phi(\mathbf{x}_t), \mathbf{w}^* \rangle_{\mathcal{H}_{RB}} = \langle \phi(\mathbf{x}_t), \hat{\rho} \rangle_{\mathcal{H}_U}. \quad (35)$$

## 4.2. Theoretical Error Analysis

We claim that the FWF is a closed-form optimal nonlinear filter in an approximate universal space, so where does error from the FWF come from? First, it is important to remember that we can only calculate the FWF solution in a finite dimensional RKHS, so the space  $\mathcal{H}_{RB}$  and therefore  $\mathcal{H}_U$  is only universal as  $D$  approaches infinity. This deficiency of  $\mathcal{H}_U$  is a source of error. In [5] error bounds for the approximation made by  $\mathcal{H}_B$  to the universal Gaussian kernel is given. Second, we still need to select the Gaussian kernel size, which in FWF only affects the precision of the results for finite number of samples. Third, since we are quantifying the joint distribution between pairs of samples projected into an RKHS and taking their mean, implicitly we are assuming that the system we are modeling is strictly stationary. Any deviation from this strictly stationary assumption can cause error. Fourth, of course there can be numerical error associated with conditioning of the  $U_M$  matrix.

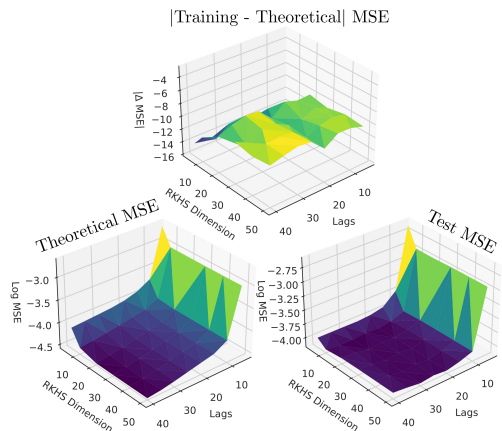


**Fig. 2.** |Training - Theoretical| MSE in log scale (Top), Theoretical MSE (left), and Test MSE (right) as a function of  $D$  and  $L$  for prediction of Mackey-Glass time series. Note the change in scale in the top plot. Kernel size is 0.25

In [22] a theoretical MMSE for the solution in  $\mathcal{H}_R$  is given with the equation

$$\mathbb{E}[|Z - \mathbb{E}[Z|X_t, t \in T]|^2] = \mathbb{E}[|Z|^2] - \langle \rho_z, \rho_z \rangle_{\mathcal{H}_R}. \quad (36)$$

We can extend this theoretical MMSE to  $\mathcal{H}_U$  by measuring the distance between the projection of  $Z$  into  $\mathcal{H}_U$  and  $Z$  in a similar manner to equation (36)

$$\mathbb{E}[|Z - \mathbb{E}[Z|\mathcal{H}_B(X_t, t \in T)]|^2] = \mathbb{E}[|Z|^2] - \langle \rho, \rho \rangle_{\mathcal{H}_U}. \quad (37)$$

This equation gives the MMSE for the solution in the finite dimensional RKHS  $\mathcal{H}_U$  even before we start make predictions with the solution. Since the projection of  $Z$  in  $\mathcal{H}_U$  is orthogonal we just need to estimate the difference between the power of the desired response and its projection in  $\mathcal{H}_U$ . This is markedly different from KAF and other filtering methods, where we have to evaluate the error in the training, which is always complex and is a function of the dynamics of learning. Therefore, discounting numerical error we can say that all the sources of error mentioned above are combined in the inner product calculation of the space  $\mathcal{H}_U$ . This means improving the error is an issue of designing correctly  $\mathcal{H}_U$  and therefore  $\mathcal{H}_{RB}$ . As an example, since the kernel size is a continuous variable, (37) can be used to estimate the optimal kernel size for the application under study.

Due to the analytical solution, the MSE on the training set should be very close to the theoretical MMSE for a given choice of the hyper-parameters: kernel size,  $L$ , and dimension  $D$ . Figure 2 shows the theoretical MMSE, the absolute difference between theoretical and calculated MSE in the training set, and the test set MSE as a function of parameters for prediction on the nonlinear chaotic Mackey-Glass time series with a kernel size of 0.25. As can be expected the larger the number of lags and the dimension of the explicit RKHS, the smaller is the error. This figure also shows that the training set MSE follows the theoretical error almost exactly for a large range of hyper parameter values. Figure 2 also shows the test set MSE as function of  $D$  and  $L$ . We can observe that the test set performance for large delays and number of eigenfunctions flattens, which is explained by overtraining. Since the FWF is a linear model, techniques for model order estimation [33] can be applied to improve generalization, but we leave this to future work.

## 5. EXPERIMENTS

Throughout these experiments we will compare the FWF solution derived above in two important applications: nonlinear mapping of one time series into another (as required in system identification) and in nonlinear time series prediction. The models used for comparison are Gaussian Process Regression (GPR) [37], Kernel Least-Mean Squares (KLMS) [19], Extended Kernel Recursive Least-Squares (KRLS) [20], Kernel Ridge Regression (KRR) [9], and Augmented Space Linear Model (ASLM) [24], which is a linear model in the joint space of the data and desired response, improving slightly the performance of the Wiener solution.

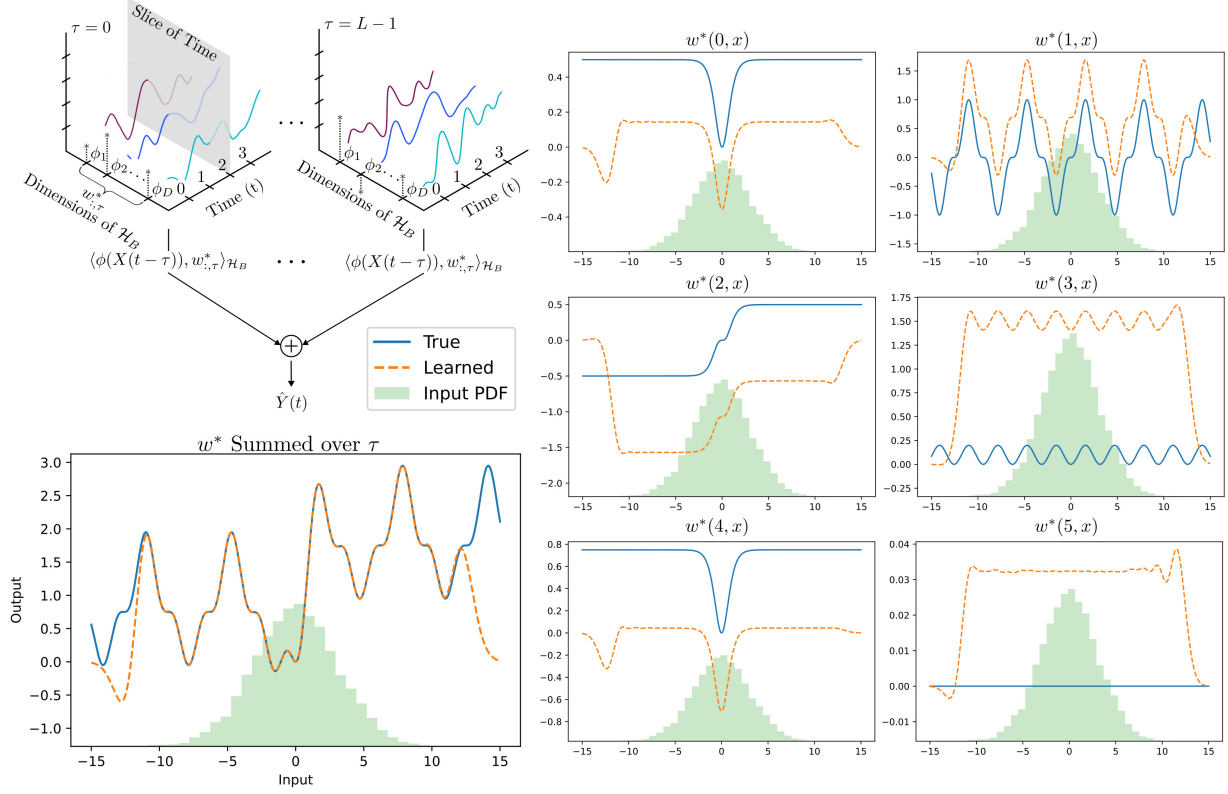


**Fig. 3.** Depiction of the FWF in finite dimensional RKHS (top left), Visualization of the solution learned by the FWF on the strictly stationary task (bottom left and right).

### 5.1. Strictly Stationary System and Function Recovery

In this section we will apply the methods to a signal that we know follows the strictly stationary assumptions made by the FWF. we will also probe the function learned by the FWF giving insight into how the FWF can learn functions that create the input data, which is very important for applications in system identification. Finally, we will compare the performance of the FWF with the other methods on this task.

First, we discuss the system used in this experiment. We first generate white Gaussian noise,  $X(n)$ , constructed by randomly sampling the distribution,  $\mathcal{N}(0, \pi)$ . We will use this white noise as the input to the models. The model output  $D(n)$  is created by applying a nonlinear mapping to  $X(n)$ ,

$$D(n) = 0.5\tanh(X(n))^2 + \sin(X(n-1))^3 + 0.5\tanh(X(n-2))^3 + 0.2\sin(X(n-3))^2 + 0.75\tanh(X(n-4))^2. \quad (38)$$

It's interesting to note that since  $\mathcal{H}_{RB}$  maintains both time and space indices we can examine more closely what functions the FWF actually learns and recover a difference equation describing the function learned by the FWF. In linear filtering, one can interpret the output of a linear system as applying a series of transformations (in this case simple scalar

multiplications) to individual samples and then summing up the result of these transformations. The difference in the FWF is that these transformations are no longer restricted to scalar multiplications. Since the FWF works with collections of functions, rather than collections of scalars, the transformations applied to each sample can be any transformation which can be described as a linear functional in  $\mathcal{H}_B$ .

In order to make this more concrete consider a window of time mapped to  $\mathcal{H}_{RB}$ ,  $\phi(x_n)$ . Each column of  $\phi(x_n)$  corresponds to the mapping of a scalar to a function in  $\mathcal{H}_B$ . We can create a tensor representation of the vector  $\mathbf{w}^*$  by folding the vector into a  $D \times L$  rank two tensor which we will denote as  $w_{d,\tau}^*$ . Note that  $d = 1, \dots, D$  and  $\tau = 0, \dots, L-1$ .

$$w_{d,\tau}^* = \begin{bmatrix} \mathbf{w}_1^* & \mathbf{w}_{D+1}^* & \dots & \mathbf{w}_{(L-1)D+1}^* \\ \vdots & \vdots & \dots & \vdots \\ \mathbf{w}_D^* & \mathbf{w}_{2D}^* & \dots & \mathbf{w}_{LD}^* \end{bmatrix}_{D \times L} \quad (39)$$

where  $\mathbf{w}_n^*$  is the  $n$ th element in the vector  $\mathbf{w}^*$ . In this form its clear to see that each column of  $w_{d,\tau}^*$  represents a transformation to be applied to each sample in a time window. Now equipped with this representation the extension of the difference equation given by the FWF is

$$\hat{Y}(n) = \sum_{\tau=0}^{L-1} \langle w_{:, \tau}^*, \phi(X(n - \tau)) \rangle_{\mathcal{H}_B} \quad (40)$$

$$= \langle \mathbf{w}^*, \phi(\mathbf{x}_n) \rangle_{\mathcal{H}_B}.$$

Here  $w_{:, \tau}^*$  is a column of the tensor depicted in (39). Each inner product in the sum over the lags can represent any linear functional in  $\mathcal{H}_B$ .

This idea is depicted visually in the top left quadrant of figure 3. The right half of figure 3 shows the  $L$  functions (one for each value of  $\tau$ ) found by the FWF with input signal  $X(n)$  and desired signal  $D(n)$ . The green histograms show the PDF of the training set (scaled for visualization). We observe that in regions covered in the training set the functions learned by the FWF are vertically shifted versions of the true functions given in the difference equation. However, when these shifted versions are summed together they converge to the true difference equation given in (38). Its also interesting that the FWF outputs a flat line for values of  $\tau$  which are larger than the true memory depth of the system.

We can think of these functions as “modes” akin to the modes found in Koopman theory [15]. The solution given by the FWF is just a sum over these modes. This interpretation of the functions learned by the FWF provides the ability to extract modes learned by the FWF and gives added explainability to the method.

Now we will compare the performance of the FWF with the methods mentioned above on this task. Each method was tested with 5 different training and testing windows at each value of  $N$ . The average test set MSE is shown in figure 4 with error bars depicting the variance of test set MSE across the different training and testing windows. For each method a search across a range of kernel sizes was performed, and the best results for each method are shown. The FWF provides a clear performance boost over the other methods on this task. The nonlinearity is not static, so the KAF have difficulties in approximating the system well. Nevertheless, this suggests that if the strict stationary assumptions made by the FWF are met, then its performance may be better than the other the nonlinear filtering methods. Moreover, we get immediately information of the time functions learned by the FWF at each lag. In later experiments we will see that if the signals do not follow this assumption the FWF is still comparable in terms of performance to the other nonlinear methods.

## 5.2. Lorenz Mapping

The Lorenz system is governed by a well known set of nonlinear equations introduced in [32]. In this experiment the models are given the  $X$  component of the Lorenz equations as input, and asked to predict the  $Z$  component 5 samples in the future. As in the previous experiment 5 different training and testing windows for each value of  $N$  were used. A grid

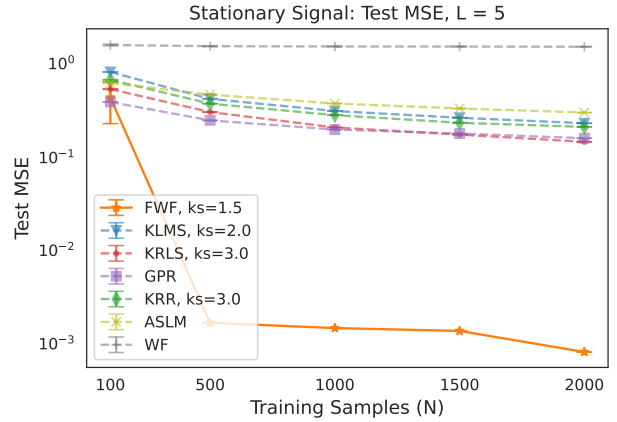


**Fig. 4.** Comparison of test set MSE as a function of number of training samples on the strictly stationary task.  $L = 5, D = 30$ .

search for kernel size was done for each kernel method and the best kernel size was selected. Figure 6 shows the result at the kernel size with the best MSE. The number of lags for each method was 20. The number of dimensions in  $\mathcal{H}_B$  was 50.

We see that FWF performance is comparable to that of KRLS and GPR, and better than KLMS, KRR and ASLM, despite the use of a finite dimensional RKHS and a strict stationary assumption, which is not fulfilled in these experiments. Moreover, at low numbers of samples the FWF tends to do better than KRLS or GPR, showing it is quite data efficient.

In figure 5 the average train and test MSE across 5-folds from the FWF is shown as a function of number of dimensions  $D$  of the RKHS. We see that beyond 20 the number of dimensions has little effect on the performance of the FWF. This could be expected since the eigenvalue spectrum of the Gaussian kernel falls off quite fast. Interestingly, the test MSE does not increase with the dimension of the space, which can be related by the orthogonality of the bases. This figure also shows that the model overfits because the test set performance is slightly higher than the training performance (the scale is logarithmic).

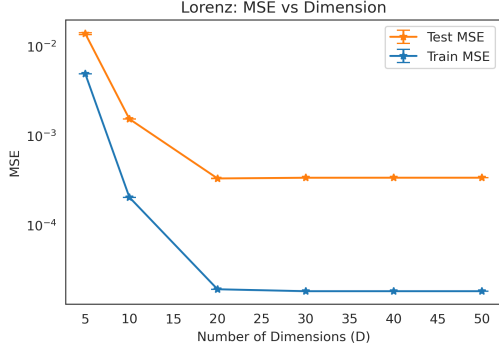


**Fig. 5.** Train and Test MSE as a function of the number of dimensions (D) in  $\mathcal{H}_U$ . Number of lags is 20, kernel size is 0.75, and number of training samples is 2000. Note the log scale for the MSE.

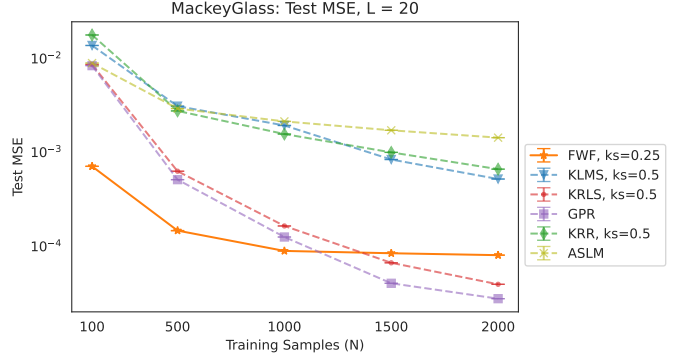


**Fig. 7.** Comparison of test set MSE as a function of Number of training samples for prediction of Mackey-Glass.

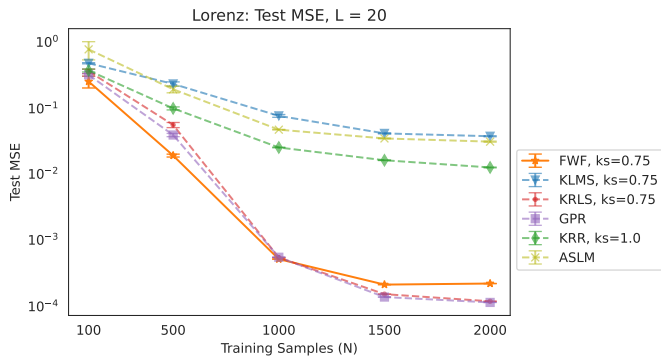


**Fig. 6.** Comparison of test set MSE as a function of number of training samples on Lorenz.

### 5.3. Mackey-Glass Prediction

In this experiment the models are tasked with prediction of the Mackey-Glass time series. Again, 5 different training and testing windows for each value of N were used. A grid search for kernel size was done for each kernel method, and the best results are shown in figure 7. The number of lags for each method was 20. The dimension of  $\mathcal{H}_B$  was 50. Again we see for low number of samples the FWF is superior, however given enough training samples the FWF performs worse than KRLS and GPR. This may be related to the low amplitude ripple in the data that is continuously changing and that represents a non-stationarity.

### 5.4. Noisy Mackey-Glass Prediction

In this section we test the same methods as before on the task of prediction of the Mackey-Glass time series with a noisy input signal. We add noise sampled from Gaussian distributions with different standard deviations (0,0.01,0.05,0.1,0.2). Again 5-fold cross validation is used with a test signal length of 300 examples. Figure 8 shows the comparative performance of these methods as the level of noise is increased. The dimension of  $\mathcal{H}_B$  was 30. We observe that, as expected, performance degrades with higher noise levels, and improves across all models with larger training sets. The FWF seems to be more sensitive to noise for smaller training sets, but follows closely the KRLS and GPR for larger number of training samples.

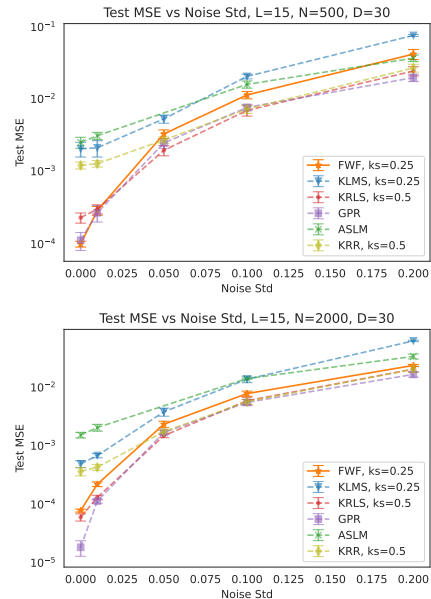


**Fig. 8.** Comparison of test set MSE as a function of standard deviation of noise for prediction of Mackey-Glass with 500 train examples (Top) and 2000 training examples (bottom).

## 5.5. Sun Spot Prediction

In this section we test the same methods, but on the sun spot data set. The goal in this task is to use the number of sun spots in the previous  $L$  days, to predict the number of sun spots which will occur on the next day. The data set was normalized to norm 1 for all the methods. We show the MSE using again 5-fold cross validation with a test signal size of 300. In this case the FWF starts with an higher error than the others for 250 samples, but converged to the performance of the best methods after 500 samples.

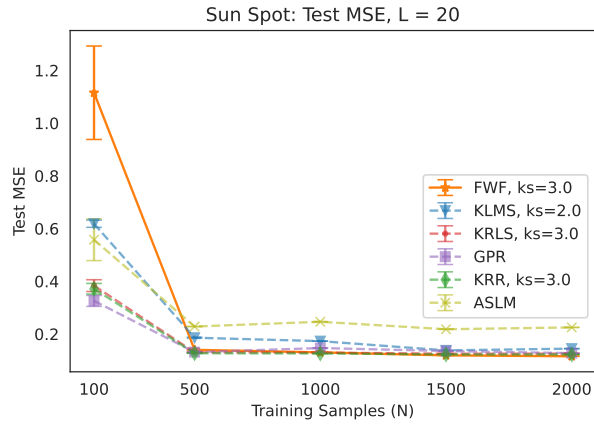


**Fig. 9.** Comparison of test set MSE as a function of of number of training samples for prediction of Sun Spot. Dimension of  $\mathcal{H}_B$  is 50.

Method	Training	Evaluation
FWF	$\mathcal{O}(NDL) + \mathcal{O}((DL)^2 N)$	$\mathcal{O}(2DL)$
KLMS	$\mathcal{O}(N)$	$\mathcal{O}(N)$
KRLS	$\mathcal{O}(N^2)$	$\mathcal{O}(N)$
ASLM	$\mathcal{O}(L^2 N) + \mathcal{O}(LN)$	$\mathcal{O}(L) + \mathcal{O}(\log(N))$
KRR	$\mathcal{O}(N^3)$	$\mathcal{O}(N^3)$
GPR	$\mathcal{O}(N^3)$	$\mathcal{O}(N^3)$

**Table 1.** Computational Complexity Comparison: D (dimension of  $\mathcal{H}_B$ ), N (number of training samples), L(number of lags)

## 6. DISCUSSION

In summary, this work extended the idea of the Wiener filter to a space nonlinearly related to the input space, yielding a closed-form solution to the MMSE problem. In order to find this MMSE solution, we must solve the system of equations resulting from the functional Wiener equation given in (30). The solution utilizes a formulation of the Wiener solution in a linear RKHS described in [22]. The extension is done in an explicit finite dimensional RKHS,  $\mathcal{H}_{RB}$ , which is nonlinearly related to the data space and utilizes a data dependent kernel in  $\mathcal{H}_U$ . The solution, to the functional Wiener Filter is given in (35), however we have to assume ergodicity in our

approach. The first conclusion is that the FWF can be interpreted as an FIR, but nonlinear transformations may be applied to each sample. We can extract the transformations applied by the FWF to each sample giving added explainability to the model. We believe that further research is needed to test the limitations of the FWF for system identification tasks. In experiments, it is shown that the performance of the FWF is comparable to that of other nonlinear regression methods such as KRLS and GPR, with gains in performance for small number of training samples and on a synthetic data set which we know follows the assumptions made by the FWF. We summarize in Table I the computational complexity of all the methods employed in the tests. As it is quite clear the computation complexity of the FWF is constant and much smaller than any of the other approaches. Effectively, it is of the same complexity as the Wiener solution for a filter order of  $D \cdot L$  as can be expected. This simplifies tremendously the application of KAF for online applications for edge computing.

Although the FWF belongs to the KAF family, its principles are totally different and represent a fresh approach to exploit the linear structure of the Hilbert space for computation. The linear model is very well understood in signal processing and control theory, but it can not compete with the versatility of nonlinear models, as the neural network revolution clearly demonstrated. The price paid by nonlinear modeling is that adaptation of parameters is non-convex, and full of local minima which brings brittleness in application. RKHS theory allows for universal approximations with convex optimal solutions named CULMS (convex universal learning machines)[23]. However, a weak link in the KAF approach is the linear (or worse) growth in the function model in RKHS, which can be traced to the definition of the RKHS domain (pairs of data samples), and the error associated with iterative gradient-based solutions. The FWF defines a kernel that preserves the time structure of the random process (or multivariate random variable) i.e., the inner product becomes now data dependent. We submit that this idea of designing the kernel with the statistics of the data is the best way for kernel design, an open problem in KAF.

How to operate effectively with data dependent kernels has been largely absent in the literature, only specific applications have been published for kernel regression [30] and for theoretical analysis [11]. This is a true advance in this paper, the development of a theory to extend nonlinear modeling in RKHS using a fixed number of parameters. We started with the MMSE problem that is crucial in statistics and time series analysis. Our solution is still limited to finite dimensional kernels, which we call explicit kernels because they truncate the eigenspectrum of universal kernels such as the Gaussian or the Laplacian kernels. In these spaces the kernel operators can be defined as quadratic forms, which allows much more flexibility than the kernel trick, because we can operate with individual dimensions of the RKHS. We claim that the MMSE solution is possible because we can estimate di-

rectly from data the correntropy along each dimension of the space (i.e moment-wise correntropy). Our previous attempt of utilizing the correntropy RKHS for MMSE, also a data dependent kernel, failed because the kernel trick is only capable of operating on pairs of columns of the tensor operator. We had to employ clustering on the training set samples to create models that would approximate the optimal solution [4], which did not generalize well.

The FWF goes beyond this “tweak” and develops a principled approach to MMSE in an explicit kernel RKHS. An analytic solution was developed and although not universal, the performance is on par with the state of the art KAF filters with much less computation, and added explainability. We expect that this approach will be quite fruitful for other stochastic signal processing applications. We summarize below the differences between the traditional KAF approach and the new data dependent approach proposed in the paper.

First, the FWF is not a search based solution, it is a analytical solution. Second, the error in the FWF comes from its assumption of stationarity and the truncation of the Gaussian kernel, not from the search method. Third, the KAF solution utilizes the kernel trick and therefore can be calculated in an infinite dimensional space. While this is a theoretical advantage, it produces functional models that increase with the training data. The use of the  $U$  operator in this derivation of the FWF solution prevents a direct generalization to an infinite dimensional RKHS, but also fixes the model size regardless of the number of training examples used.

There are other contributions of this work beyond the closed-form solution. We develop a data-dependent RKHS in  $\mathcal{H}_U$  which contains information about the correlation structure intrinsic to the data used to construct  $K_U$ . While we do not give an eigendecomposition of this kernel directly, we do describe how to take inner products in  $\mathcal{H}_U$ . Since this RKHS is data-dependent the “rules” described as statistical averages with respect to different dimensions of the input space are contained within the eigenstructure of the space. This in theory could lead to very computationally efficient kernels tuned to deal with data from a specific distribution. More research needs to be conducted to see if this is indeed the case. Other uses for data-dependent kernels have been described, for example, [10] uses a cross-density kernel to quantify dependence between random processes. There may be different RKHSs like  $\mathcal{H}_U$  which need to be explored.

## Appendices

### A. WHY DO WE NEED MOMENT-WISE CORRENTROPY?

In this work we have proposed a method to solve the Functional Wiener equation in (30) in a finite dimensional RKHS.

We do this by extending the idea of a covariance function  $R(s, t)$ , to a moment-wise correntropy function  $U_{d_1, d_2}(s, t)$ . However, if one is familiar with the KAF literature this is not the most obvious extension of  $R(s, t)$ . The most obvious extension to a nonlinear space would be the correntropy function described in [18]. This correntropy function,  $V(s, t)$ , paired with the Gaussian kernel,  $G_\sigma$ , is defined as

$$\begin{aligned} V(s, t) &= \mathbb{E}[G_\sigma(X_s, X_t)] \\ G_\sigma(x, y) &= e^{\left(\frac{-||x-y||_2^2}{2\sigma^2}\right)}. \end{aligned} \quad (41)$$

In [18] it is shown that this function is PSD and therefore defines a data-dependent RKHS which we will call  $\mathcal{H}_V$ . This definition of correntropy is the expected value between kernel evaluations centered at a time series indexed with two different time indices. This means  $V$  is a measure of the average correlation across all spatial dimensions of  $G_\sigma$  and does not contain the inter-dimensional correlations that the  $U$  function in equation (15) describes. An attempt to use the correntropy function in (41) in order to define a data-dependent RKHS in which to solve the Wiener equation is made in [4] with limited success. The question is why is  $V$  insufficient to give an analytical solution to a nonlinear filter?

Separable Hilbert spaces can be isomorphic only if they have the same number of dimensions. A key crux of the argument used by Parzen is that the linear span of a time series in  $L^2$  is congruent to  $\mathcal{H}_R$ , suggesting an isomorphism between these two spaces exists. This congruence allows one to solve the MMSE solution in  $\mathcal{H}_R$  with the guarantee that this solution is equivalent to the optimal solution in the linear span of a time series in  $L^2$ .  $\mathcal{H}_V$  is a data-dependent kernel and measures correlations between a time series at different time indices, but it forms an  $L$  dimensional RKHS, therefore it can not be congruent to  $\mathcal{H}_G$  (the gaussian RKHS). There cannot be a one-to-one inner product preserving mapping between RKHSs with different number of dimensions. Therefore, we cannot hope to give an analytical solution in  $\mathcal{H}_V$  equivalent to picking some functional in  $\mathcal{H}_G$  which is the representation of the desired mapping function. In fact, many different time series are equivalent in terms of  $V$ , because  $V$  averages over all spatial dimensions. This means that permutations of the same spectral coefficients will result in the  $V$  function giving the same scalar value.

When we use  $\mathcal{H}_U$  we form a RKHS with the same number of dimensions as  $\mathcal{H}_{RB}$  so we do not encounter this issue.  $\mathcal{H}_U$  and  $\mathcal{H}_{RB}$  share the same congruent relationship that  $L^2(\{X_t\})$  and  $\mathcal{H}_R$  share. The operator  $U^{\frac{1}{2}}$  defines an isomorphism between the two spaces. This is why Parzen’s arguments could be readily extended using  $\mathcal{H}_U$ , but are not so easily extended to  $\mathcal{H}_V$ .

## References

- [1] Nachman Aronszajn. “The theory of reproducing kernels and their applications”. In: *Cambridge Philos. Soc. Proc.* 39 (1943), pp. 133–153.
- [2] Liangjun Chen, Hua Qu, and Jihong Zhao. “Generalized correntropy induced loss function for deep learning”. In: *2016 International Joint Conference on Neural Networks (IJCNN)*. 2016, pp. 1428–1433. DOI: 10.1109/IJCNN.2016.7727366.
- [3] Benjamin Colburn, Luis G. Sanchez Giraldo, and Jose C. Principe. *The Functional Wiener Filter*. 2022. arXiv: 2301.00291 [eess.SP].
- [4] Benjamin Colburn, Jose C. Principe, and Luis G. Sanchez Giraldo. *An Alternate View on Optimal Filtering in an RKHS*. 2023. arXiv: 2312.12318 [cs.LG].
- [5] Andrew Cotter, Joseph Keshet, and Nathan Srebro. *Explicit Approximations of the Gaussian Kernel*. 2011. arXiv: 1109.4603 [cs.AI].
- [6] D. Duttweiler and T. Kailath. “RKHS approach to detection and estimation problems–IV: Non-Gaussian detection”. In: *IEEE Transactions on Information Theory* 19.1 (1973), pp. 19–28. DOI: 10.1109/TIT.1973.1054928.
- [7] D. Duttweiler and T. Kailath. “RKHS approach to detection and estimation problems–V: Parameter estimation”. In: *IEEE Transactions on Information Theory* 19.1 (1973), pp. 29–37. DOI: 10.1109/TIT.1973.1054949.
- [8] Marc Genton. “Classes of Kernels for Machine Learning: A Statistics Perspective.” In: *Journal of Machine Learning Research* 2 (Jan. 2001), pp. 299–312. DOI: 10.1162/15324430260185646.
- [9] Arthur E. Hoerl and Robert W. Kennard. “Ridge Regression: Biased Estimation for Nonorthogonal Problems”. In: *Technometrics* 42.1 (2000), pp. 80–86. ISSN: 00401706. URL: <http://www.jstor.org/stable/1271436> (visited on 09/05/2023).
- [10] Bo Hu and Jose C. Principe. *The Cross Density Kernel Function: A Novel Framework to Quantify Statistical Dependence for Random Processes*. 2022. arXiv: 2212.04631 [cs.LG].
- [11] Arthur Jacot, Franck Gabriel, and Clement Hongler. “Neural Tangent Kernel: Convergence and Generalization in Neural Networks”. In: *Advances in Neural Information Processing Systems*. Ed. by S. Bengio et al. Vol. 31. Curran Associates, Inc., 2018. URL: [https://proceedings.neurips.cc/paper\\_files/paper/2018/file/5a4be1fa34e62bb8a6ec6b91d2462f5a-Paper.pdf](https://proceedings.neurips.cc/paper_files/paper/2018/file/5a4be1fa34e62bb8a6ec6b91d2462f5a-Paper.pdf).
- [12] T Kailath and D Duttweiler. “An RKHS approach to detection and estimation problems-part III: Generalized innovations representations and a likelihood-ratio formula”. In: *IEEE Trans. Inf. Theory* 18.6 (1972), pp. 730–745.
- [13] T Kailath and H Weinert. “An RKHS approach to detection and estimation problems-part II: Gaussian signal detection”. In: *IEEE Trans. Inf. Theory* 21.1 (1975), pp. 15–23.
- [14] Rodney A. Kennedy and Parastoo Sadeghi. *Hilbert Space Methods in Signal Processing*. Cambridge University Press, 2013. DOI: 10.1017/CBO9780511844515.
- [15] B O Koopman and J V Neumann. “Dynamical systems of continuous spectra”. en. In: *Proc. Natl. Acad. Sci. U. S. A.* 18.3 (Mar. 1932), pp. 255–263.
- [16] Kan Li and Jose Principe. “Transfer Learning in Adaptive Filters: The Nearest-Instance-Centroid-Estimation Kernel Least-Mean-Square Algorithm”. In: *IEEE Transactions on Signal Processing* PP (Sept. 2017), pp. 1–1. DOI: 10.1109/TSP.2017.2752695.
- [17] Kan Li and Jose C. Principe. *No-Trick (Treat) Kernel Adaptive Filtering using Deterministic Features*. 2019. arXiv: 1912.04530 [cs.LG].
- [18] W Liu, P Pokharel, and J Principe. “Correntropy: Properties and Applications in Non Gaussian Signal Processing”. In: *IEEE Trans. Sig. Proc* 55 (2007), pp. 5286–5298.
- [19] Weifeng Liu, Puskar Pokharel, and Jose Principe. “The Kernel Least-Mean-Square Algorithm”. In: *Signal Processing, IEEE Transactions on* 56 (Mar. 2008), pp. 543–554. DOI: 10.1109/TSP.2007.907881.
- [20] Weifeng Liu et al. “Extended Kernel Recursive Least Squares Algorithm”. In: *IEEE Transactions on Signal Processing* 57.10 (2009), pp. 3801–3814. DOI: 10.1109/TSP.2009.2022007.
- [21] Michel Loeve. *Probability theory*. 3rd ed. Mineola, NY: Dover Publications, July 1955.
- [22] Emanuel Parzen. “An Approach to Time Series Analysis”. In: *The Annals of Mathematical Statistics* 32.4 (1961), pp. 951–989. DOI: 10.1214/aoms/1177704840. URL: <https://doi.org/10.1214/aoms/1177704840>.
- [23] Jose C. Principe and Badong Chen. “Universal Approximation with Convex Optimization: Gimmick or Reality? [Discussion Forum]”. In: *IEEE Computational Intelligence Magazine* 10.2 (2015), pp. 68–77. DOI: 10.1109/MCI.2015.2405352.
- [24] Zhengda Qin et al. “Augmented Space Linear Models”. In: *IEEE Transactions on Signal Processing* 68 (2020), pp. 2724–2738. DOI: 10.1109/TSP.2020.2987053.

[25] Stefan Ragnarsson and Charles F. Van Loan. *Block Tensor Unfoldings*. 2011. arXiv: 1101.2005 [math.NA].

[26] Ali Rahimi and Benjamin Recht. “Random Features for Large-Scale Kernel Machines”. In: *Advances in Neural Information Processing Systems*. Ed. by J. Platt et al. Vol. 20. Curran Associates, Inc., 2007. URL: [https://proceedings.neurips.cc/paper\\_files/paper/2007/file/013a006f03dbc5392effeb8f18fda755-Paper.pdf](https://proceedings.neurips.cc/paper_files/paper/2007/file/013a006f03dbc5392effeb8f18fda755-Paper.pdf).

[27] Murali Rao et al. “A Test of Independence Based on a Generalized Correlation Function”. In: *Signal Process*. 91.1 (Jan. 2011), pp. 15–27. ISSN: 0165-1684. DOI: 10.1016/j.sigpro.2010.06.002. URL: <https://doi.org/10.1016/j.sigpro.2010.06.002>.

[28] Peter J. Schmid. “Dynamic mode decomposition of numerical and experimental data”. In: *Journal of Fluid Mechanics* 656 (2010), pp. 5–28. DOI: 10.1017/S0022112010001217.

[29] Bernhard Schölkopf and Alexander J. Smola. *Learning with kernels : support vector machines, regularization, optimization, and beyond*. Adaptive computation and machine learning. MIT Press, 2002. URL: <http://www.worldcat.org/oclc/48970254>.

[30] James B. Simon. *On Kernel Regression with Data-Dependent Kernels*. 2022. arXiv: 2209.01691 [cs.LG].

[31] Alastair Spence. “On the convergence of the Nystrom method for the integral equation eigenvalue problem”. en. In: *Numer. Math. (Heidelberg)* 25.1 (Mar. 1975), pp. 57–66.

[32] *Spline models for observational data*. 1990.

[33] P. Stoica and Y. Selen. “Model-order selection: a review of information criterion rules”. In: *IEEE Signal Processing Magazine* 21.4 (2004), pp. 36–47. DOI: 10.1109/MSP.2004.1311138.

[34] Norbert Wiener. *Extrapolation, Interpolation, and Smoothing of Stationary Time Series*. New York: Wiley, 1949.

[35] Norbert Wiener. *Generalized Harmonic Analysis*. Sitzungber. Akad. Wiss. Berlin, 1930.

[36] Norbert Wiener. *Ueber eine Klasse singulärer Integralgleichungen*. Sitzungber. Akad. Wiss. Berlin, 1931.

[37] Christopher Williams and Carl Rasmussen. “Gaussian Processes for Regression”. In: *Advances in Neural Information Processing Systems*. Ed. by D. Touretzky, M.C. Mozer, and M. Hasselmo. Vol. 8. MIT Press, 1995. URL: [https://proceedings.neurips.cc/paper\\_files/paper/1995/file/7cce53cf90577442771720a370c3c723-Paper.pdf](https://proceedings.neurips.cc/paper_files/paper/1995/file/7cce53cf90577442771720a370c3c723-Paper.pdf).

[38] Jian-Wu Xu et al. “A Reproducing Kernel Hilbert Space Framework for Information-Theoretic Learning”. In: *IEEE Transactions on Signal Processing* 56.12 (2008), pp. 5891–5902. DOI: 10.1109/TSP.2008.2005085.

[39] Jian-Wu Xu et al. “An Explicit Construction Of A Reproducing Gaussian Kernel Hilbert Space”. In: *2006 IEEE International Conference on Acoustics Speech and Signal Processing Proceedings*. Vol. 5. 2006, pp. V–V. DOI: 10.1109/ICASSP.2006.1661340.

[40] Changjiang Yang, Ramani Duraiswami, and Larry S Davis. “Efficient Kernel Machines Using the Improved Fast Gauss Transform”. In: *Advances in Neural Information Processing Systems*. Ed. by L. Saul, Y. Weiss, and L. Bottou. Vol. 17. MIT Press, 2004. URL: [https://proceedings.neurips.cc/paper\\_files/paper/2004/file/85353d3b2f39b9c9b5ee3576578c04b7-Paper.pdf](https://proceedings.neurips.cc/paper_files/paper/2004/file/85353d3b2f39b9c9b5ee3576578c04b7-Paper.pdf).

[41] Songlin Zhao, BD Chen, and Jose Principe. “Kernel adaptive filtering with maximum correntropy criterion”. In: *Proceedings of the International Joint Conference on Neural Networks* (July 2011), pp. 2012–2017. DOI: 10.1109/IJCNN.2011.6033473.